

BIVARIATE GAMMA DISTRIBUTIONS FOR MULTISENSOR SAR IMAGES

F. Chatelain and J.-Y. Tournéret

* IRIT/ENSEEIH/TéSA, 2 rue Charles Camichel, BP 7122, 31071 Toulouse cedex 7, France

{florent.chatelain, jean-yves.tourneret}@enseeiht.fr

ABSTRACT

This paper addresses the problem of estimating the parameters of a family of bivariate gamma distributions whose margins have different shape parameters. These distributions are interesting to detect changes in two synthetic radar aperture (SAR) images acquired by different sensors and having different numbers of looks. The estimators based on the maximum likelihood method and the method of moments are studied for these distributions. An application to change detection is finally discussed.

Index Terms— Gamma distributions, maximum likelihood estimation, synthetic aperture imaging, multisensor systems

1. INTRODUCTION

Combining informations acquired from multiple sensors has become very popular in many signal and image processing applications. One motivation for this fusion is that the limitations of a specific kind of sensors can be compensated by the use of complementary sensors. This is particularly true for earth observation applications as noted in [1, 2]. This paper addresses the problem of change detection in synthetic aperture radar (SAR) images acquired by multiple sensors (characterized by different numbers of looks).

We consider two multi-date remote sensing images of the same scene I , the reference, and J , the secondary image after an abrupt change, like a natural disaster. The change detection problem consists of determining the map of the changed pixels from a similarity measure. The key element of the change detection problem, is therefore the estimation of the correlation coefficient between the images. This is usually done with an estimation window in the neighborhood of each pixel. In order to estimate the change map with a good resolution one needs the smallest estimation window. However, this leads to estimations which may not be robust enough. In order to perform high quality estimations with a small number of samples, we propose to introduce a priori knowledge about the image statistics. In the case of power radar images, it is well known that the pixels are marginally distributed according to gamma distributions [3]. Therefore, multivariate gamma distributions (having univariate gamma margins) seem good candidates for the robust estimation of the correlation coefficient between radar images. When multi-date power radar images are acquired from different sensors, the numbers of looks associated with the different images can be different. As the number of looks is the shape parameter of the gamma distribution, this leads to study multivariate gamma distributions whose margins have different shape parameters.

A family of multivariate gamma distributions has been recently defined by S. Bar Lev and P. Bernardoff [4, 5]. These distributions are defined from an appropriate moment generating function. Their

margins are distributed according to univariate gamma distributions having the same shape parameter. They have recently shown interesting properties for registration and change detection in SAR images acquired by the same sensor (i.e. for images having the same number of looks) [6, 7]. This paper studies a new family of bivariate gamma distributions whose margins have different shape parameters referred to as multisensor bivariate gamma distributions (MuBGDs). The application of MuBGDs to change detection in SAR images is also investigated.

This paper is organized as follows. Section 2 recalls important results on monosensor bivariate gamma distributions (MoBGDs). Section 3 defines the family of MuBGDs considered for change detection in multisensor SAR images. Section 4 studies the maximum likelihood estimator (MLE) and the estimator of moments for the unknown parameters of MuBGDs. Simulation results illustrating the performance of MuBGDs for parameter estimation and change detection are presented in Section 5. Conclusions and perspectives are finally reported in Section 6.

2. MONOSENSOR BIVARIATE GAMMA DISTRIBUTIONS

2.1. Definition

A random vector $\mathbf{X} = (X_1, X_2)^T$ is distributed according to a monosensor bivariate gamma distribution (MoBGD) on \mathbb{R}_+^2 with shape parameter q and scale parameter P if its moment generating function, or Laplace transform, is defined as follows [5]:

$$\psi_{q,P}(\mathbf{z}) = \mathbb{E} \left(e^{-\sum_{i=1}^2 X_i z_i} \right) = [P(\mathbf{z})]^{-q}, \quad (1)$$

where $\mathbf{z} = (z_1, z_2)$, $q \geq 0$ and $P(\mathbf{z}) = 1 + p_1 z_1 + p_2 z_2 + p_{12} z_1 z_2$ is a so-called affine polynomial whose coefficients satisfy the following conditions

$$p_1 > 0, p_2 > 0, p_1 p_2 - p_{12} > 0. \quad (2)$$

It is important to note that the conditions (2) ensure that (1) is the Laplace transform of a probability distribution defined on $[0, \infty[^2$. By setting $z_2 = 0$ (resp. $z_1 = 0$) in (1), we obtain the Laplace transform of X_1 (resp. X_2), which is clearly a univariate gamma distribution with shape parameter q and scale parameter p_1 (resp. p_2), denoted as $X_1 \sim \Gamma(q, p_1)$ (resp. $X_2 \sim \Gamma(q, p_2)$). Thus, both margins of \mathbf{X} are univariate gamma distributions with the same shape parameter q . The reader is invited to consult [6] and [7] for having more details regarding the properties of MoBGDs.

2.2. Probability density function

The probability density function (pdf) of an MoBGD can be expressed as follows (see [8, p. 436] for a similar result)

$$f_{2D}(\mathbf{x}) = \exp \left(-\frac{p_2 x_1 + p_1 x_2}{p_{12}} \right) \frac{x_1^{q-1} x_2^{q-1}}{p_{12}^q \Gamma(q)} f_q(c x_1 x_2) \mathbb{I}_{\mathbb{R}_+^2}(\mathbf{x}),$$

This work was supported by CNES and by the CNRS under MathSTIC Action No. 80/0244.

where $\mathbb{I}_{\mathbb{R}_+^2}(\mathbf{x})$ is the indicator function on $[0, \infty]^2$ ($\mathbb{I}_{\mathbb{R}_+^2}(\mathbf{x}) = 1$ if $x_1 > 0, x_2 > 0$ and $\mathbb{I}_{\mathbb{R}_+^2}(\mathbf{x}) = 0$ otherwise), $c = (p_1 p_2 - p_{12})/p_{12}^2$ and $f_q(z)$ is related to the confluent hypergeometric function ([8, p. 462]) and defined by

$$f_q(z) = \sum_{k=0}^{\infty} \frac{z^k}{k! \Gamma(q+k)}.$$

3. MULTISENSOR BIVARIATE GAMMA DISTRIBUTIONS

3.1. Definition

A random vector $\mathbf{Y} = (Y_1, Y_2)^T$ distributed according to an MuBGD is constructed as follows:

$$Y_1 = X_1, \quad Y_2 = X_2 + Z, \quad (3)$$

where

- $\mathbf{X} = (X_1, X_2)^T$ is a random vector distributed according to an MoBGD on \mathbb{R}_+^2 with shape parameter q_1 and scale parameter P , i.e. $X \sim \Gamma(q_1, P)$,
- Z is a random variable independent on \mathbf{X} and distributed according to a univariate gamma distribution $\Gamma(q_2 - q_1, p_2)$ with $q_2 > q_1$.

By using the independence property between \mathbf{X} and Z , the Laplace transform of \mathbf{Y} can be written:

$$\psi(z) = \left(1 + \sum_{i=1}^2 p_i z_i + p_{12} z_1 z_2 \right)^{-q_1} (1 - p_2 z_2)^{-(q_2 - q_1)}, \quad (4)$$

with the following conditions:

$$p_1 > 0, \quad p_2 > 0, \quad p_1 p_2 - p_{12} > 0 \quad \text{and} \quad q_2 \geq q_1. \quad (5)$$

In the bi-dimensional case, the conditions (5) ensure that (4) is the Laplace transform of a probability distribution defined on $[0, \infty]^2$.

By setting $z_1 = 0$ in (4), we observe that the random variable Y_1 is distributed according to a univariate gamma distribution with scale parameter p_1 and shape parameter q_1 . Similarly, Y_2 is distributed according to a univariate gamma distribution with scale parameter p_2 and shape parameter q_2 . Therefore the random vector \mathbf{Y} is said to be distributed according to an MuBGD with scale parameter P and shape parameter $\mathbf{q} = (q_1, q_2)$, denoted as $\mathbf{Y} \sim \Gamma(\mathbf{q}, P)$. This definition assumes that the first univariate margin Y_1 has a shape parameter q_1 smaller than q_2 without loss of generality. Note that an MuBGD reduces to an MoBGD for $q_1 = q_2$.

3.2. Probability density function

By construction, the pdf of a bivariate vector $\mathbf{Y} \sim \Gamma(\mathbf{q}, P)$ denoted as $f_{\mathbf{Y}}(\mathbf{y})$ is the convolution between $f_{\mathbf{X}}(\mathbf{x})$ and the pdf $f_Z(z)$ of $Z \sim \Gamma(q_2 - q_1, p_2)$. Straightforward computations leads to the following expression:

$$f_{\mathbf{Y}}(\mathbf{y}) = \left(\frac{p_1 p_2}{p_{12}} \right)^{q_1} \frac{y_1^{q_1-1} y_2^{q_2-1}}{p_1^{q_1} p_2^{q_2}} \frac{e^{-\left[\frac{p_2}{p_{12}} y_1 + \frac{p_1}{p_{12}} y_2\right]}}{\Gamma(q_2) \Gamma(q_1)} \times \Phi_3 \left(q_2 - q_1; q_2; c \frac{p_{12}}{p_2} y_2, c y_1 y_2 \right), \quad (6)$$

where $c = (p_1 p_2 - p_{12})/p_{12}^2$ and where Φ_3 is the Horn function. The Horn function is one of the twenty convergent confluent hypergeometric series of order two, defined as [9]:

$$\Phi_3(a; b; x, y) = \sum_{m,n=0}^{\infty} \frac{(a)_m}{(b)_{m+n} m! n!} x^m y^n, \quad (7)$$

where $(a)_m$ is the Pochhammer symbol such that $(a)_0 = 1$ and $(a)_{k+1} = (a+k)(a)_k$ for any positive integer k .

3.3. Moments

The moments of $\mathbf{Y} = (Y_1, Y_2)^T = (X_1, X_2 + Z)^T$ are directly obtained from those of \mathbf{X} and Z . By using the independence between Z and \mathbf{X} , the following results can be obtained:

$$\begin{aligned} E[Y_i] &= q_i p_i, \quad \text{var}(Y_i) = q_i p_i^2, \quad i = 1, 2, \\ \text{cov}(Y_1, Y_2) &= \text{cov}(X_1, X_2) = q_1 (p_1 p_2 - p_{12}), \\ r(Y_1, Y_2) &= \frac{\text{cov}(Y_1, Y_2)}{\sqrt{\text{var}(Y_1)} \sqrt{\text{var}(Y_2)}} = \sqrt{\frac{q_1}{q_2}} \frac{p_1 p_2 - p_{12}}{p_1 p_2}. \end{aligned}$$

It is interesting to note that the conditions (2) ensure that the correlation coefficient r satisfy the constraint $0 \leq r \leq \sqrt{q_1/q_2}$. We introduce the normalized correlation coefficient defined by

$$r'(Y_1, Y_2) = \sqrt{\frac{q_2}{q_1}} r(Y_1, Y_2) = \frac{p_1 p_2 - p_{12}}{p_1 p_2},$$

such that $0 \leq r' \leq 1$. For known values of the shape parameters q_1 and q_2 , a MuBGD is fully characterized by the parameter vector $\boldsymbol{\theta} = (E[Y_1], E[Y_2], r'(Y_1, Y_2))$, since $\boldsymbol{\theta}$ and (p_1, p_2, p_{12}) are related by a one-to-one transformation.

4. PARAMETER ESTIMATION

The following notations are used in the rest of the paper

$$m_1 = E[Y_1], \quad m_2 = E[Y_2], \quad r' = r(Y_1, Y_2) \sqrt{\frac{q_2}{q_1}},$$

inducing $\boldsymbol{\theta} = (m_1, m_2, r')$. This section addresses the problem of estimating the unknown parameter vector $\boldsymbol{\theta}$ from n vectors $\mathbf{Y} = (\mathbf{Y}^1, \dots, \mathbf{Y}^n)$, where $\mathbf{Y}^i = (Y_1^i, Y_2^i)$ is distributed according to an MuBGD with parameter vector $\boldsymbol{\theta}$. Note that the parameters q_1 and q_2 are assumed to be known here, as in most practical applications. However, this assumption could be relaxed.

4.1. Maximum Likelihood Method

4.1.1. Principles

The maximum likelihood (ML) method can be applied to \mathbf{Y} since a closed-form expression of its pdf is available. In this particular case, after removing the terms which do not depend on $\boldsymbol{\theta}$, the log-likelihood function can be written

$$\begin{aligned} l(\mathbf{Y}; \boldsymbol{\theta}) &= -n q_1 \log(1 - r') - n q_1 \log m_1 - n q_2 \log m_2 \\ &\quad - n \frac{q_1}{m_1(1 - r')} \bar{Y}_1 - n \frac{q_2}{m_2(1 - r')} \bar{Y}_2 \\ &\quad + \sum_{i=1}^n \log \Phi_3 \left(q_2 - q_1; q_1; d Y_2^i, c Y_1^i Y_2^i \right). \end{aligned} \quad (8)$$

where $c = \frac{r' q_1 q_2}{m_1 m_2 (1 - r')^2}$, $d = \frac{r' q_1}{m_1 (1 - r')}$ and $\bar{Y}_1 = \frac{1}{n} \sum_{i=1}^n Y_1^i$, $\bar{Y}_2 = \frac{1}{n} \sum_{i=1}^n Y_2^i$ are the sample means of Y_1 and Y_2 . By differentiating the log-likelihood with respect to $\boldsymbol{\theta}$, the following MLE of m_2 is easily derived

$$\widehat{m}_{2\text{ML}} = \bar{Y}_2. \quad (9)$$

The MLEs of m_1 and r' are obtained by replacing m_2 by $\widehat{m}_{2\text{ML}}$ in (8) and minimizing the resulting log-likelihood $l(\mathbf{Y}; (m_1, \widehat{m}_{2\text{ML}}, r')$ with respect to m_1 and r' . This last minimization is achieved by using a constrained ($m_1 > 0$ and $r' \in [0, 1]$) quasi-Newton method, since an analytical expression of the log-likelihood gradient is available. It is important to note that the MLE of m_1 differs from \bar{Y}_1 in the general case. Finally, the MLE of the correlation coefficient r is deduced by functional invariance as

$$\widehat{r}_{\text{ML}} = \sqrt{\frac{q_1}{q_2}} \widehat{r}'_{\text{ML}}.$$

4.1.2. Numerical evaluation of the Horn function Φ_3

Some series representation in terms of special functions are useful to compute hypergeometric series of order two [10]. For the Horn function Φ_3 defined in (7), the following expansion is particularly useful:

$$\Phi_3(a; b; x, y) = \sum_{n=0}^{\infty} \frac{y^n}{(b)_n n!} {}_1F_1[a, b+n, x],$$

where ${}_1F_1$ is the confluent hypergeometric series of order one, i. e. ${}_1F_1[a, b, x] = \sum_{n=0}^{\infty} \frac{(a)_n}{(b)_n n!} x^n$. This confluent hypergeometric series ${}_1F_1[a, b, x]$ can be expressed as follows [11]:

$${}_1F_1[a, b, x] = \frac{\Gamma(b)}{\Gamma(a)} e^x x^{a-b} \sum_{i \geq 0} \frac{(b-a)_i (1-a)_i}{i! x^i} F_\gamma(x; i+b-a), \quad (10)$$

where $F_\gamma(x; \nu)$ is the cumulative distribution function of a univariate gamma distribution with shape parameter ν and scale parameter 1. Note that the summation in (10) is finite since $a \geq 1$ is an integer. This yields the following expression of Φ_3 :

$$\begin{aligned} \Phi_3(a; b; x, y) &= \frac{\Gamma(b)}{\Gamma(a)} e^x x^{a-b} \sum_{n=0}^{\infty} \frac{(y/x)^n}{n!} \\ &\times \sum_{i \geq 0} \frac{(b+n-a)_i (1-a)_i}{i! x^i} F_\gamma(x; i+b+n-a). \end{aligned} \quad (11)$$

where the last summation ($i \geq 0$) is finite. Equation (11) provides a numerically stable way of evaluating $\Phi_3(a; b; x, y)$ for large values of x and y . When (x, y) is close to $(0, 0)$, the definition of Φ_3 in (7) will be preferred.

4.1.3. Performance

The properties of the ML estimator $\widehat{m}_{2\text{ML}}$ can be easily derived from the properties of the univariate gamma distribution $\Gamma(q_2, p_2)$. This estimator is obviously unbiased, convergent and efficient. However, the performance of $\widehat{m}_{1\text{ML}}$ and \widehat{r}_{ML} are more difficult to study. Of course, the MLE is known to be asymptotically unbiased and asymptotically efficient, under mild regularity conditions. Thus, the mean square error of the estimates can be approximated for large data records by the Cramer-Rao lower bound (CRLB). For unbiased estimators, the CRLB is obtained by inverting the Fisher information matrix. The computation of this matrix requires to determine the negative expectations of second-order derivatives (with respect to m_1, m_2 and r) of $l(\mathbf{Y}; \boldsymbol{\theta})$ in (8). Closed-form expressions for the expectations are difficult to obtain because of the term $\log \Phi_3$. In such situation, it is very usual to approximate the expectations by using Monte Carlo methods. This will provide interesting approximations of the ML mean square errors (MSEs) (see simulation results of Section 5).

4.2. Method of Moments

In order to appreciate the performance of the MLE, the following estimators of moments are investigated:

$$\widehat{m}_{1\text{Mo}} = \bar{X}_1, \quad \widehat{m}_{2\text{Mo}} = \bar{X}_2, \quad (12)$$

$$\widehat{r}_{\text{Mo}} = \frac{\sum_{i=1}^n (X_1^i - \bar{X}_1)(X_2^i - \bar{X}_2)}{\sqrt{\sum_{i=1}^n (X_1^i - \bar{X}_1)^2} \sqrt{\sum_{i=1}^n (X_2^i - \bar{X}_2)^2}}. \quad (13)$$

Note that $\widehat{m}_{2\text{Mo}} = \widehat{m}_{2\text{ML}}$ and that \widehat{r}_{Mo} is the usual empirical correlation coefficient. The asymptotic performance of the estimator $\widehat{\boldsymbol{\theta}}_{\text{Mo}} = (\widehat{m}_{1\text{Mo}}, \widehat{m}_{2\text{Mo}}, \widehat{r}_{\text{Mo}})$ can be derived by imitating the results of [12] derived in the context of time series analysis (see also [13]).

5. SIMULATION RESULTS

Many simulations have been conducted to validate the previous theoretical results. This section presents some experiments obtained with a vector $\mathbf{Y} = (Y_1, Y_2)^T$ distributed according to a MuBGD whose Laplace transform is (4).

5.1. Generation of synthetic data

According to the definition given in Section 3.1, a vector \mathbf{Y} distributed according to an MuBGD can be generated by adding a random variable Z distributed according to a univariate gamma distribution to a random vector \mathbf{X} distributed according to an MoBGD. The generation of a vector \mathbf{X} whose Laplace transform is (1) has been described in [6] and is summarized below:

- simulate $2q$ independent multivariate Gaussian vectors of \mathbb{R}^2 denoted as Z^1, \dots, Z^{2q} with means $(0, 0)$ and the 2×2 covariance matrix $C = (c_{i,j})_{1 \leq i, j \leq 2}$ with $c_{i,j} = r \frac{|i-j|}{2}$,
- compute the k th component of $\mathbf{X} = (X_1, X_2)$ as $X_k = \frac{m_k}{2q} \sum_{1 \leq i \leq 2q} (Z_k^i)^2$, where Z_k^i is the k th component of Z^i .

5.2. Estimation performance

The first simulations compare the performance of the estimators corresponding to the method of moments and the maximum likelihood (ML) method as a function of the sample size n . Note that the possible values of n corresponds to the numbers of pixels of squared windows of size $(2p+1) \times (2p+1)$, where $p \in \mathbb{N}$. These values are appropriate to the change detection problem. The number of Monte Carlo runs is 200 for all figures presented in this section. The other parameters for this example are $m_1 = 150$, $m_2 = 200$, $q_1 = 1$ (number of looks of the first image) and $q_2 = 2$ (number of looks of the second image). Figure 1 shows the MSEs of the estimated normalized correlation coefficient for $r' = 0.8$. The circle curves correspond to the estimator of moments whereas the triangle curves correspond to the MLE. This figure shows the interest of the ML method, which is much more efficient for this problem than the method of moments. Note that the theoretical asymptotic MSEs of both estimators are also depicted (continuous lines). They are clearly in good agreement with the estimated MSEs, even for small values of n . Finally, these figures show that "reliable" estimates of r can be obtained for values of n larger than 9×9 , i.e. even for relatively small window sizes. The results regarding the estimation of (m_1, m_2) confirm this result but are not reported here for brevity.

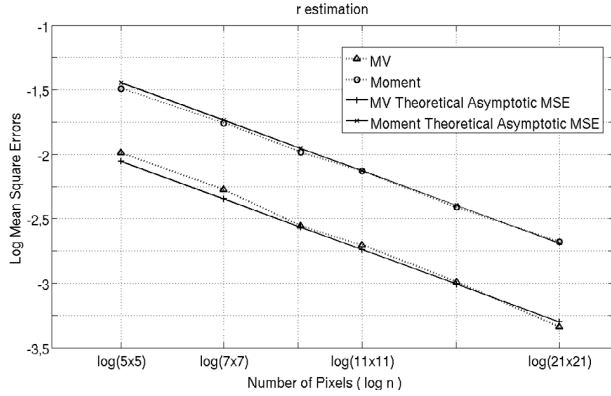


Fig. 1. log MSEs versus log n for parameter r ($r' = 0.8$, $q_1 = 1$, $q_2 = 2$).

5.3. Detection performance

This section considers synthetic vectors $\mathbf{x} = (x_1, x_2)^T$ (coming from 762×292 synthetic images) distributed according to MuBGDs with $r = 0.3$ and $r = 0.7$, modelling the absence and presence of changes, respectively. The correlation coefficient r of each bivariate vector $\mathbf{x}^{(i,j)} = (x_1^{(i,j)}, x_2^{(i,j)})^T$ (for $1 \leq i \leq 762$, $1 \leq j \leq 292$) is estimated locally from pixels belonging to windows of size $n = (2p + 1) \times (2p + 1)$ centered around the pixel of coordinates (i, j) in the two analyzed images. The change detection problem is addressed by using the following binary hypothesis test:

$$\begin{aligned} H_0 \quad (\text{absence of change}) : \quad & \hat{r} > \lambda, \\ H_1 \quad (\text{presence of change}) : \quad & \hat{r} \leq \lambda, \end{aligned} \quad (14)$$

where λ is a threshold depending on the probability of false alarm (PFA) and \hat{r} is an estimator of the correlation coefficient (obtained from the method of moments or the maximum likelihood principle). The performance of the change detection strategy (14) can be defined by the two following probabilities [14, p. 34]

$$\begin{aligned} P_D &= P[\text{accepting } \mathcal{H}_1 | \mathcal{H}_1 \text{ is true}] = P[\hat{r} < \lambda | \mathcal{H}_1 \text{ is true}], \\ P_{FA} &= P[\text{accepting } \mathcal{H}_1 | \mathcal{H}_0 \text{ is true}] = P[\hat{r} > \lambda | \mathcal{H}_0 \text{ is true}]. \end{aligned}$$

Thus, a pair (P_{FA}, P_D) can be defined for each value of λ . The curves representing P_D as a function of P_{FA} are called receiver operating characteristics (ROCs) and are classically used to assess detection performance [14, p. 38].

The ROCs for the change detection problem (14) are depicted on figures 2(a) and 2(b) for two different values of the shape parameters corresponding to $(q_1 = 1, q_2 = 2)$ and $(q_1 = 1, q_2 = 5)$. The results are presented for two window sizes (9×9) and (21×21) . The ML estimator clearly outperforms the moment estimator for these examples. It is also interesting to note that the change detection is better when the numbers of looks of the two images are closer.

6. CONCLUSIONS

This paper presented a new family of bivariate gamma distributions for multisensor SAR images. Estimation algorithms based on the maximum likelihood principle and the methods of moments have been studied to estimate the parameters of these distributions. These

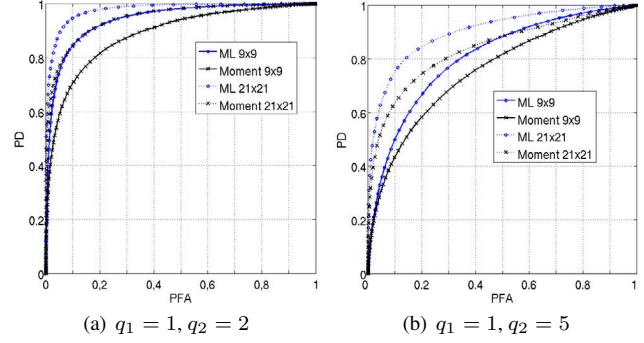


Fig. 2. ROCs for synthetic data with different shape parameters.

distributions showed good properties for the detection of changes in radar images with different numbers of looks.

7. ACKNOWLEDGMENTS

The authors would like to thank J. Inglada and G. Letac for fruitful discussions regarding change detection and multivariate gamma distributions. They are also very grateful to F. Colavecchia and G. Gasaneo for providing important informations regarding the implementation of the Horn function.

8. REFERENCES

- [1] J. Inglada, "Similarity measures for multisensor remote sensing images," in *Proc. IEEE IGARSS-02*, (Toronto, Canada), pp. 104–106, June 2002.
- [2] J. Inglada and A. Giros, "On the possibility of automatic multi-sensor image registration," *Transactions on Geoscience and Remote Sensing*, vol. 42, pp. 2104–2120, Oct. 2004.
- [3] T. F. Bush and F. T. Ulaby, "Fading characteristics of panchromatic radar backscatter from selected agricultural targets," *IEEE Trans. Geoscience and Remote Sensing*, vol. 13, no. 4, pp. 149–157, 1975.
- [4] S. B. Lev, D. Bshouty, P. Enis, G. Letac, I. L. Lu, and D. Richards, "The diagonal natural exponential families and their classification," *J. of Theoret. Prob.*, vol. 7, pp. 883–928, 1994.
- [5] P. Bernardoff, "Which multivariate Gamma distributions are infinitely divisible?," *Bernoulli*, 2006.
- [6] F. Chatelain, J.-Y. Tourneret, A. Ferrari, and J. Inglada, "Bivariate gamma distributions for image registration and change detection," *IEEE Trans. Image Processing*, 2006, submitted.
- [7] F. Chatelain, J.-Y. Tourneret, J. Inglada, and A. Ferrari, "Parameter estimation for multivariate gamma distributions. Application to image registration," in *Proc. EUSIPCO-06*, (Florence, Italy), sep 2006.
- [8] S. Kotz, N. Balakrishnan, and N. L. Johnson, *Continuous Multivariate Distributions*, vol. 1. New York: Wiley, 2nd ed., 2000.
- [9] F. O. A. Erdlyi, W. Magnus and F. Tricomi, *Higher Transcendental Functions*, vol. 1. New York: Krieger, 1981.
- [10] F. D. Colavecchia and G. Gasaneo, "f1: a code to compute Appell's F_1 hypergeometric function," *Computer Physics Communications*, vol. 157, pp. 32–38, feb 2004.
- [11] K. E. Muller, "Computing the confluent hypergeometric function, $M(a, b, x)$," *Numerische Mathematik*, vol. 90, pp. 179–196, Nov. 2001.
- [12] B. Porat and B. Friedlander, "Performance analysis of parameter estimation algorithms based on high-order moments," *International Journal of adaptive control and signal processing*, vol. 3, pp. 191–229, 1989.
- [13] F. Chatelain, A. Ferrari, and J.-Y. Tourneret, "Parameter estimation for multivariate mixed Poisson distributions," in *Proc. IEEE ICASSP-06*, vol. IV, (Toulouse, France), pp. 17–20, May 2006.
- [14] H. L. Van Trees, *Detection, Estimation, and Modulation Theory: Part I*. New York: Wiley, 1968.